Journal of Molecular Graphics and Modelling 28 (2010) 506–512

Contents lists available at ScienceDirect

Journal of Molecular Graphics and Modelling

journal homepage: www.elsevier.com/locate/JMGM

Molecular docking study for the prediction of enantiodifferentiation of chiral styrene oxides by octakis(2,3-di-*O*-acetyl-6-*O*-*tert*-butyldimethylsilyl)-γ-cyclodextrin

Natthapol Issaraseriruk [a,b], Aroonsiri Shitangkoon [a,b], Thammarat Aree [a,b,*]

[a] Department of Chemistry, Faculty of Science, Chulalongkorn University, Bangkok 10330, Thailand
[b] Center for Petroleum, Petrochemicals, and Advanced Materials, Chulalongkorn University, Bangkok 10330, Thailand

ARTICLE INFO

Article history:
Received 4 August 2009
Received in revised form 22 November 2009
Accepted 27 November 2009
Available online 3 December 2009

Keywords:
γ-Cyclodextrin
Enantiodifferentiation
Inclusion complexation
Molecular docking
PM3
Styrene oxides

ABSTRACT

A molecular docking study, using molecular mechanics calculations with AutoDock and semi-empirical PM3 calculations, was used to help predict the enantiodiscrimination of mono-substituted styrene oxides by octakis(2,3-di-*O*-acetyl-6-*O*-*tert*-butyldimethylsilyl)-γ-cyclodextrin (DIACTGCD), through the differences in the interaction energies and inclusion geometries. The small differences in the binding free energy values ($\Delta\Delta G$) obtained from AutoDock do not show any significant enantiodifferentiation, whereas structure re-optimization with the PM3 algorithm results in larger binding energy differences ($\Delta\Delta E$). All DIACTGCD–styrene oxide inclusion complexes have binding energies in the range of −13.62 to −3.83 kcal mol^{-1}, indicating that the host–guest interactions involved are hydrophobic and van der Waals forces between the C=O acetyl group, the O2/O3/O4 atoms of DIACTGCD and the substituents/epoxide group of styrene oxides. The effect of the same substituent position on the inclusion geometry is similar for all styrene oxides entirely embedded at or near the central DIACTGCD cavity. The degrees of enantiodiscrimination are: $o > m > p$ for Cl-, CH_3- and CF_3-enantiomers and $o > p > m$ for Br-, F- and NO_2-enantiomers. The molecular docking results suggest that the complexation between styrene oxides and DIACTGCD depends on the type and position of the substituents on the aromatic ring. The high discriminatory ability exhibited by DIACTGCD against enantiomeric styrene oxides could potentially serve as a chiral selector, for example in chromatographic separation.

1. Introduction

α-, β- and γ-Cyclodextrins (CDs) are torus-like macrocycles comprised of six, seven and eight D-glucopyranose units, respectively [1]. CDs and their derivatives form inclusion complexes with a wide variety of guest molecules, including isomers and enantiomers, and have been widely used as a chiral stationary phase (CSP) in chromatography for chiral separations (reviewed in [2–9]). The enantioseparation of CD derivatives strongly depends on the CD cavity size, the type and the degree of substitution of the substituents on the primary hydroxyls O6-H and on the secondary hydroxyls O2-H and O3-H of the glucose units of CD [4]. Amongst the CD CSPs, permethylated β-CD and 6-*O*-*tert*-butyldimethylsilyl-β-CD derivatives are extensively applied in enantiomeric gas chromatography (GC), whereas 6-*O*-*tert*-butyldimethylsilyl-γ-CD derivatives are rare and deserve further investigations [8].

Enantiopure styrene oxides are of interest because they are used as chiral building blocks for the synthesis of a variety of pharmaceutical products and as intermediates for the synthesis of more complex chiral organic compounds [10,11].

Over the past 20 years, there have been many molecular modeling studies on the chromatographic separations of enantiomers aimed at both the rationalization and prediction of experimental results. Two comprehensive reviews by Lipkowitz have been published for the five types of CSPs [12] and for type III CSPs, particularly on CDs [13]. For the CD inclusion complexation, different host CDs and guest enantiomers have been investigated by various molecular modeling methods, e.g. molecular mechanics, molecular dynamics and Monte Carlo [12,13]. The given examples are for rationalization of the GC separation on 6-*O*-*tert*-butyldimethylsilyl-β-CD-based CSPs [14–16] and for prediction of chiral separations of β-CD and its derivatives as chiral selectors [17–20]. However, a general explanation and guideline for the prediction of the existent or observed enantioselectivity cannot be established.

* Corresponding author at: Department of Chemistry, Faculty of Science, Chulalongkorn University, Bangkok 10330, Thailand. Tel.: +66 2 218 7584; fax: +66 2 254 1309.
E-mail address: thammarat.aree@gmail.com (T. Aree).

1093-3263/$ – see front matter © 2009 Elsevier Inc. All rights reserved.
doi:10.1016/j.jmgm.2009.11.005

In this study, we perform molecular docking simulations, using (i) a molecular mechanics method with AutoDock and (ii) the semi-empirical Parametric Model 3 (PM3) method, to systematically investigate and predict enantiorecognition of styrene oxides by octakis(2,3-di-*O*-acetyl-6-*O*-*tert*-butyldimethylsilyl)-γ-cyclodextrin (DIACTGCD). Because DIACTGCD has a slightly larger cavity size and is less symmetric, it may better anchor and discriminate chiral guests when compared with the corresponding derivative of β-CD.

2. Computational methods

To simplify the calculations, we assumed that the guests bind primarily within the DIACTGCD cavity and hence that the enantiorecognition is mainly attributed to the distinction in structures and interaction energies of the inclusion complexes. However, it should be noted that this assumption is still controversial because some chiral separations may occur when a cavity is not available, i.e., chiral recognition by interaction with the outer CD surface, in the interstices between CD molecules. This is an analogy to the interactions with linear dextrins that have been reported recently [21–23].

2.1. Structure optimization of host DIACTGCD and guest styrene oxides

The starting atomic coordinates of DIACTGCD non-H-atoms were taken from the X-ray crystal structure of octakis(2,3,6-tri-*O*-methyl)-γ-CD [24]; all methyl C-atoms were replaced at the O2 and O3 positions with acetyl groups and at the O6 positions with *tert*-butyldimethylsilyl groups. All H-atoms were added. The structures obtained were then optimized using the PM3 method implemented in Gaussian 03 [25]. Styrene oxide (SO) and its 18 derivatives (hereafter, the abbreviations used are, for example, *o*-Br, *m*-Br and *p*-Br standing for *ortho*-, *meta*- and *para*-bromostyrene oxides, respectively) were optimized at the calculation level HF/6-31G** with Gaussian 03 [25]. The optimized structures of host and guests were used for the molecular docking calculations. The chemical structures and atom labeling of DIACTGCD and styrene oxides are given in Scheme 1.

2.2. Molecular docking simulations

Molecular docking simulations were carried out with the automated docking program, AutoDock 4.0.1 [26]. A Lamarckian Genetic Algorithm (LGA) in combination with a grid-based energy evaluation method were used for pre-calculating grid maps according to the interatomic potentials of all atom types present in the host and guest molecules, including the 12-6 Lennard–Jones potentials for van der Waals interactions and Coulomb potentials for electrostatic interactions. A grid map of dimensions

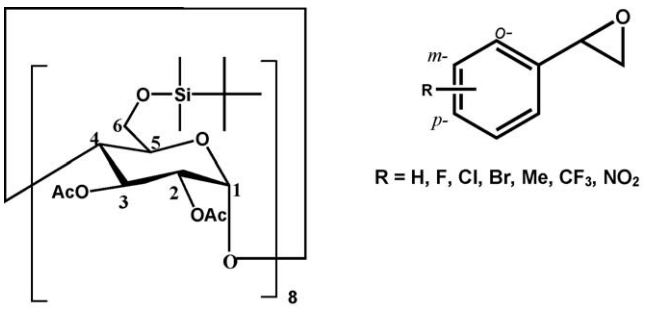

Scheme 1. Chemical structures of DIACTGCD and styrene oxide derivatives. Atomic numbering is given for the CD skeleton.

Table 1
Binding free energies at 298 K of the complexes between DIACTGCD and 19 styrene oxides obtained from molecular docking with AutoDock [26]. Units are in kcal mol^{-1}.

Analyte	%Frequency	ΔG[a]	$\Delta\Delta G$[b]
SO			
R	100	−4.18	0.00
S	100	−4.18	
o-F			
R	96	−1.25	0.28
S	100	−1.53	
m-F			
R	100	−2.63	−0.16
S	94	−2.47	
p-F			
R	84	−1.70	−0.03
S	100	−1.67	
o-Cl			
R	98	−3.91	−0.05
S	100	−3.86	
m-Cl			
R	100	−3.26	0.05
S	97	−3.31	
p-Cl			
R	86	−3.47	−0.01
S	68	−3.46	
o-Br			
R	100	−4.33	−0.06
S	99	−4.27	
m-Br			
R	85	−2.36	−0.07
S	100	−2.29	
p-Br			
R	100	−3.35	−0.05
S	99	−3.30	
o-Me			
R	100	−2.37	0.08
S	100	−2.45	
m-Me			
R	100	−0.38	−0.05
S	100	−0.33	
p-Me			
R	78	−1.80	0.02
S	97	−1.82	
o-CF_3			
R	100	−1.50	−0.24
S	81	−1.26	
m-CF_3			
R	66	−1.19	0.22
S	99	−1.41	
p-CF_3			
R	94	−1.27	−0.10
S	70	−1.17	
o-NO_2			
R	90	−2.26	0.11
S	99	−2.37	
m-NO_2			
R	74	−1.54	−0.08
S	91	−1.46	
p-NO_2			
R	94	0.04	0.02
S	50	0.02	

[a] Binding free energies derived from AutoDock 4 with standard errors of ~2.5 kcal mol^{-1}.
[b] Binding free energy difference between the complexes of the (*R*)- and (*S*)-enantiomers, $\Delta\Delta G = \Delta G_R - \Delta G_S$; negative/positive value means the elution order: (*S*) > (*R*)/(*R*) > (*S*).

15 Å × 15 Å × 15 Å, with a grid spacing of 0.375 Å, was placed to cover the DIACTGCD molecule. With the help of AutoDockTools [27], the atomic partial charges were calculated by the Gasteiger–Marsili method [28] and other docking parameters were set as default. For each guest analyte, two possible orientations, namely that the epoxy group points towards either the O2/O3 side or the O6 side in the host DIACTGCD cavity were considered as starting configurations in the docking calculations. One hundred LGA runs, each with 300 individuals in the population, were performed. Results differing by less than 1 Å in a positional root mean square deviation (rmsd) were clustered together. In each group, the lowest binding energy configuration with the highest % frequency was selected as the group representative. Since the binding free energies between the complexes of the (*R*)- and (*S*)-enantiomers obtained from AutoDock are insignificantly different, the dominating configurations of all the complexes were re-optimized to obtain the binding energy at the PM3 level using Gaussian 03 [25].

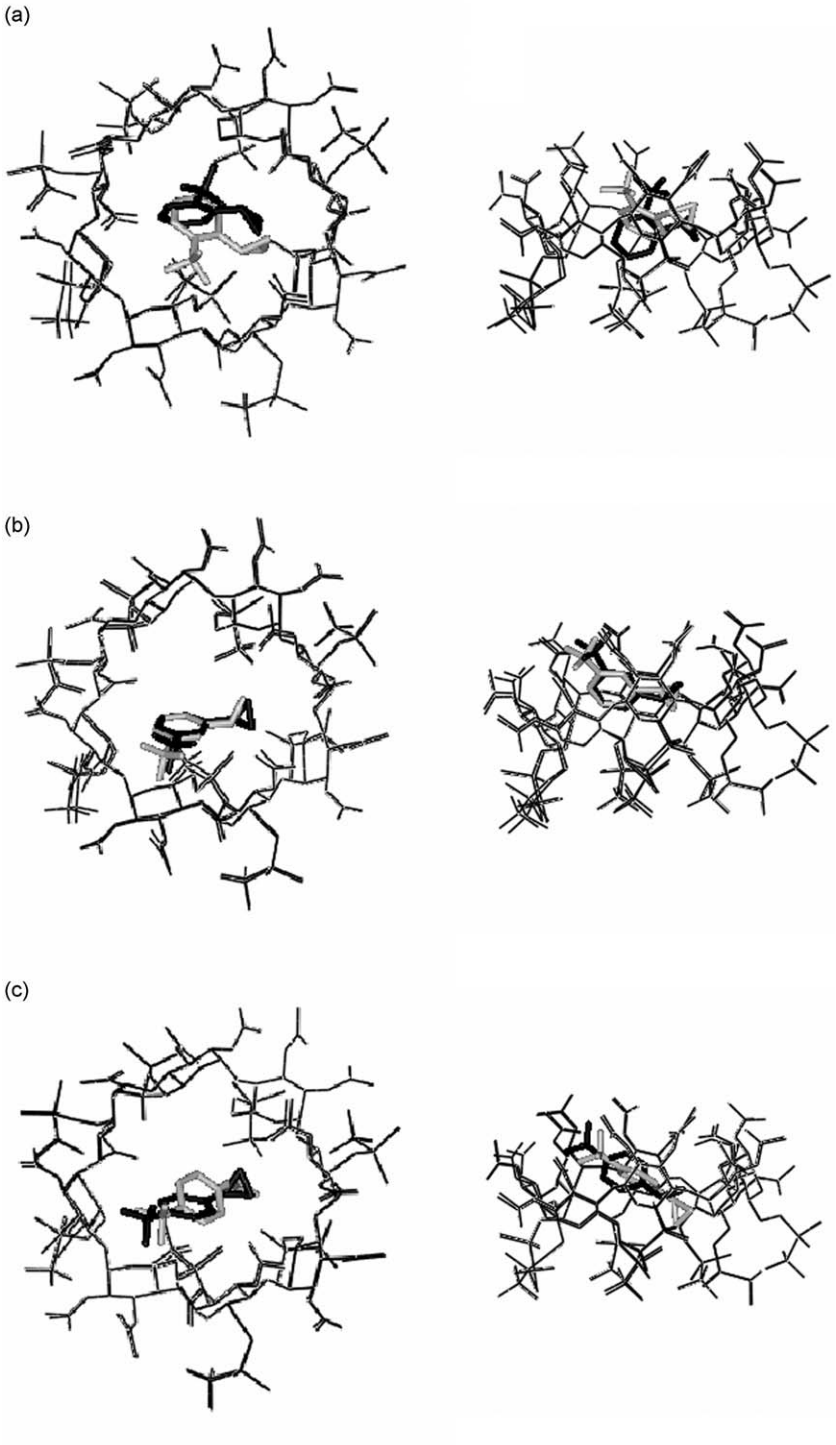

Fig. 1. Superposition of the PM3-derived most stable complexes between DIACTGCD (black wireframe) and the (*R*)- (black stick) or (*S*)- (grey stick) enantiomers of (a) *o*-CF_3, (b) *m*-CF_3 and (c) *p*-CF_3; top view on the left and side view on the right.

3. Results and discussion

3.1. Structures and binding energies of DIACTGCD–styrene oxide complexes from AutoDock

The results of molecular docking with AutoDock between DIACTGCD and the 19 styrene oxides are presented for the dominating configuration with minimum binding free energy (ΔG) in Table 1. All enantiomeric complexes have a short span of ΔG in the range of −4.33 to −0.33 kcal mol^{-1} with frequencies of 66–100%, except for the complexes of (*R*)- and (*S*)-enantiomers of *p*-NO_2 that are the least stable with ΔG of 0.04 and 0.02 kcal mol^{-1}, and frequencies of 94 and 50%, respectively. Consequently, the binding free energy differences ($\Delta\Delta G$), which range from −0.24 to 0.28 kcal mol^{-1}, are insignificant because they are about 10 times smaller than the standard error (∼2.5 kcal mol^{-1}) of the docking simulations obtained with AutoDock (Table 1). However, in the chromatographic context these small $\Delta\Delta G$ values, if valid, would be sufficient for chiral separations [29]. The insignificant differences in the binding free energy values between (*R*)- and (*S*)-enantiomers is probably because the unrealistic assumption of a rigid DIACTGCD structure used in AutoDock does not account for any DIACTGCD-induced fit conformational changes, which have been shown before to be essential for inclusion complexation [30]. Hence, the AutoDock results, with respect to the structural distinction and tendency of enantiodifferentiation, are not discussed any further here.

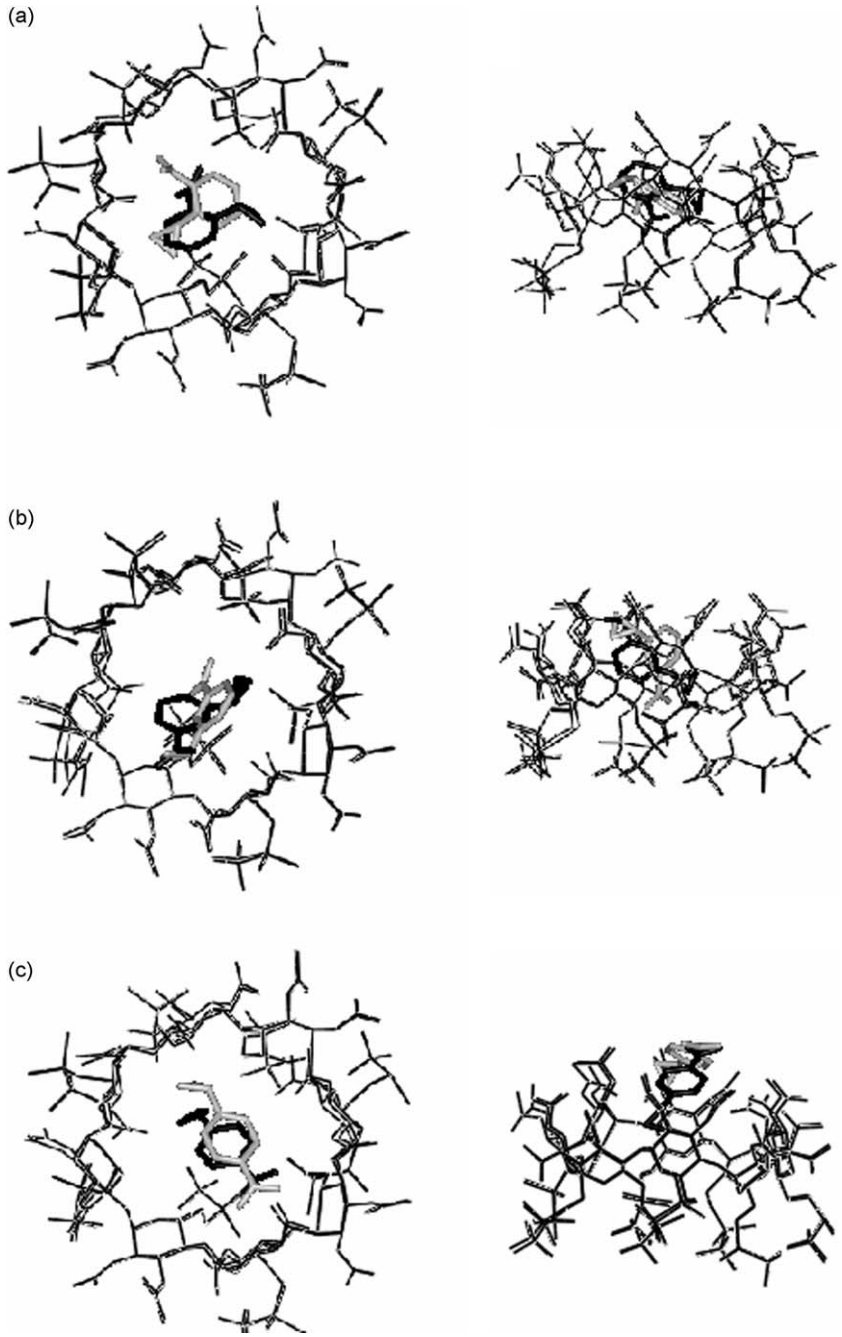

Fig. 2. Superposition of the PM3-derived most stable complexes between DIACTGCD (black wireframe) and the (*R*)- (black stick) or (*S*)- (grey stick) enantiomers of (a) *o*-NO_2, (b) *m*-NO_2 and (c) *p*-NO_2; top view on the left and side view on the right.

3.2. Structures and binding energies from PM3 calculations

Because AutoDock does not provide a meaningful $\Delta\Delta G$, as mentioned above, the alternative method of PM3 calculation was used for the evaluation of the binding energy. Full structure optimization with PM3 was performed on each of the AutoDock dominating configurations for each enantiomeric complex. The DIACTGCD structures obtained from the PM3 and AutoDock analyses are superimposable, with rmsd values within the range of 0.15–0.60 Å, except for the complexes of (*S*)-*o*-F, (*S*)-*p*-Br and (*S*)-*p*-NO_2 that have larger rmsd values of 0.84, 0.66 and 0.69 Å, respectively. As expected, the optimized structure of DIACTGCD is much distorted from a regular "round" conformation of native CDs or non-simultaneously derivatized CDs at positions 2 and 3, where the intramolecular O3···O2 hydrogen bonds exist. This is well supported by crystal structures of annular heptakis(2-*O*-methyl)-β-CD [31], heptakis(6-*O*-*tert*-butyldimethylsilyl)-β-CD [32], heptakis(2,6-di-*O*-*tert*-butyldimethylsilyl)-β-CD [31] and distorted heptakis(2-*O*-methyl-3,6-di-*O*-*tert*-butyldimethylsilyl)-β-CD [31].

Enantiodifferentiation of the complexes between DIACTGCD and styrene oxides were assessed as distinctions in inclusion geometries (Figs. 1 and 2) and binding energies (Table 2). The effect of the same substituent position on the inclusion geometry is similar for all analytes entirely embedded at or near the central DIACTGCD cavity. The (*R*)- and (*S*)-enantiomers of the *o*-substituted analytes exhibit greater differences in the inclusion geometry in the DIACTGCD cavity than do the *m*- and *p*-derivatives (Figs. 1 and 2). Hence, the DIACTGCD column has a higher discriminatory ability against the enantiomers of *o*-derivatives than that for the *m*- and *p*-derivatives. The *o*-CF_3 derivatives, with the CF_3 groups pointing towards the DIACTGCD O2/O3 side, inclines at 60° and 25° with respect to the DIACTGCD axis for the (*S*)- and (*R*)-enantiomers, respectively (Fig. 1a). By contrast, both (*R*)- and (*S*)-enantiomers of *m*-CF_3 and *p*-CF_3 are oriented similarly in the DIACTGCD cavity with the aromatic rings almost superimposed and the epoxy groups pointed in the same direction with respect to the DIACTGCD C3-H and C5-H groups (Fig. 1b and c). Similar observations are also seen for the NO_2 derivatives (Fig. 2). The corresponding illustrations of other complexes are given as supporting information, emphasizing that the styrene oxide *o*-derivatives are best enantiodifferentiated by DIACTGCD. Differences in inclusion geometries facilitating the three-point interaction are required for chiral recognition [33,34]. The positions of styrene oxides embedded at or near the central DIACTGCD cavity, as derived from the PM3 analysis in this study, are different from those of the dihydrofuranones that were reported from molecular dynamic simulations to be close to the O2/O3 side of the smaller derivatized β-CD ring [15]. Variations in the guest inclusion geometries to attain the energetically most favorable complex strongly depend on the size and shape of the host and guest molecules.

All DIACTGCD–analyte inclusion complexes have binding energies (ΔE_{bind}) and binding energy differences ($\Delta\Delta E$) in the range of −13.62 to −3.83 and −3.13 to 3.77 kcal mol^{-1}, respectively (Table 2). These relatively small but meaningful energy differences are derived on the assumption that computational errors in each enantiomeric complex are similar and so are effectively eliminated out [35]. The host–guest interactions involved are hydrophobic and van der Waals forces between the C=O acetyl group, the O2/O3/O4 atoms of DIACTGCD and the substituents/epoxide group of styrene oxides (Table 2). The (*S*)-styrene oxide complex is less stable than the (*R*)-styrene oxide complex, as shown by the ΔE_{bind} of −10.27 and −11.18 kcal mol^{-1}, respectively; giving a binding energy difference between the two enantiomeric complexes ($\Delta\Delta E$) of −0.91 kcal mol^{-1}. For enantiomeric derivatives with different substituent positions, the

Table 2
Formation energies of free DIACTGCD and 19 styrene oxides and binding energies of the complexes obtained with the PM3 method.

Analyte	E_{cpx}[a]	E_{guest}	ΔE_{bind}[a]	$\Delta\Delta E$[b]
SO				
R	−2907.09	17.66	−11.18	−0.91
S	−2906.18		−10.27	
o-F				
R	−2945.73	−25.09	−7.08	2.85
S	−2948.59		−9.93	
m-F				
R	−2945.03	−25.80	−5.67	−1.41
S	−2943.62		−4.26	
p-F				
R	−2946.56	−25.91	−7.08	1.51
S	−2948.07		−8.59	
o-Cl				
R	−2909.18	11.89	−7.51	2.55
S	−2911.73		−10.06	
m-Cl				
R	−2907.85	11.08	−5.37	−1.54
S	−2906.31		−3.83	
p-Cl				
R	−2908.31	10.96	−5.70	−0.19
S	−2909.18		−5.51	
o-Br				
R	−2893.66	26.15	−6.24	−2.21
S	−2891.44		−4.03	
m-Br				
R	−2892.79	25.47	−4.70	0.42
S	−2893.21		−5.12	
p-Br				
R	−2893.10	25.40	−4.94	1.29
S	−2894.39		−6.23	
o-Me				
R	−2914.03	9.39	−9.85	3.77
S	−2917.80		−13.62	
m-Me				
R	−2914.04	8.30	−8.78	1.62
S	−2915.66		−10.40	
p-Me				
R	−2916.28	8.22	−10.94	−1.27
S	−2915.01		−9.67	
o-CF_3				
R	−3059.04	−137.59	−7.88	−3.13
S	−3055.91		−4.75	
m-CF_3				
R	−3059.82	−140.59	−5.66	0.69
S	−3060.50		−6.35	
p-CF_3				
R	−3063.22	−140.53	−9.13	−0.44
S	−3062.78		−8.69	
o-NO_2				
R	−2911.88	12.06	−10.38	−2.66
S	−2909.22		−7.72	
m-NO_2				
R	−2913.22	8.97	−8.63	−0.87
S	−2912.35		−7.76	
p-NO_2				
R	−2911.75	9.07	−7.26	1.37
S	−2913.12		−8.63	

[a] $\Delta E_{bind} = E_{cpx} - (E_{host} + E_{guest})$; where $E_{host} = -2913.56$ kcal mol^{-1}.
[b] Binding energy difference between the complexes of the (*R*)- and (*S*)-enantiomers, $\Delta\Delta E = \Delta E_R - \Delta E_S$; negative/positive value means the elution order: (*S*) > (*R*)/(*R*) > (*S*).

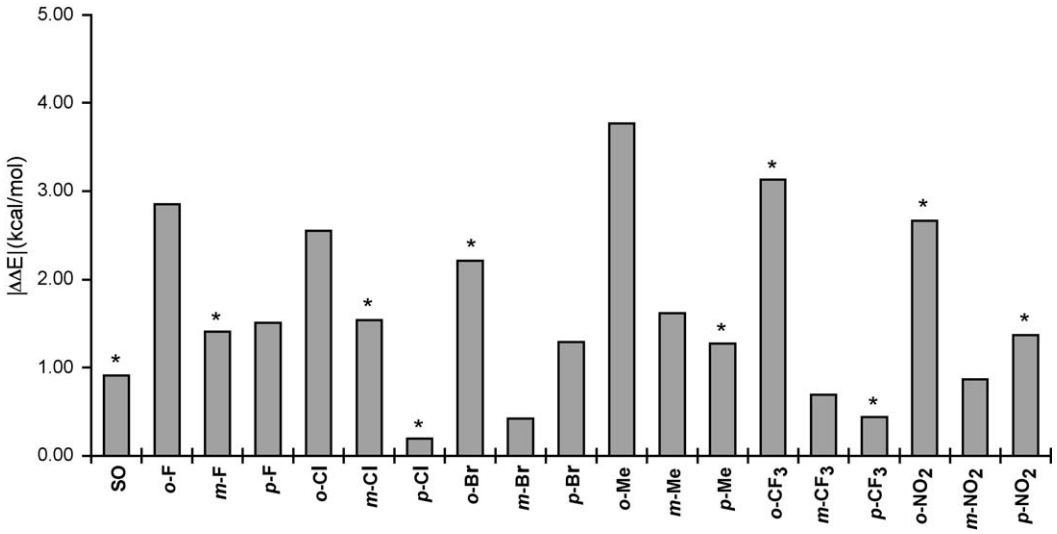

Fig. 3. Binding energy difference ($\Delta\Delta E$) between the complexes of the (*R*)- and (*S*)-enantiomers of 19 styrene oxides. All negative $\Delta\Delta E$ values are marked with a star.

enantiodifferentiation increases with increasing binding energy differences. Note that the actual positive and negative $\Delta\Delta E$ values imply the elution orders of $R > S$ and $S > R$, respectively. However, in the absence of suitable experimental data, the predicted elution orders cannot be validated here. The largest $\Delta\Delta E$ of the six complexes of the *o*-derivatives: 2.85 kcal mol^{-1} (F), 2.55 kcal mol^{-1} (Cl), −2.21 kcal mol^{-1} (Br), 3.77 kcal mol^{-1} (CH_3), −3.13 kcal mol^{-1} (CF_3) and −2.66 kcal mol^{-1} (NO_2) indicates their better recognition on the DIACTGCD when compared with the *m*- and *p*-derivatives (Table 2). Indeed, the $\Delta\Delta E$ magnitudes are in the order *o*- > *m*- > *p*- for the Cl-, CH_3- and CF_3-derivatives, whereas they are in the order *o*- > *p*- > *m*- for the Br-, F- and NO_2-derivatives (Table 2 and Fig. 3). This is different from the GC results where the tendency for enantioseparations of mono-substituent of phenylsulfoxides by 2,6-di-*O*-pentyl-3-trifluoroacetyl-, 2,6-di-*O*-pentyl-3-propionyl- and 2,6-di-*O*-pentyl-3-butyryl-γ-CDs is in the order *m*- > *o*- > *p*- [36]. The more recent GC results show that the 125 enantiomeric compounds comprising various sizes, shapes and functional groups (alcohols, lactones, aromatic, methyl branched and sulfur-containing compounds) could be separated by 2,3-di-*O*-methoxymethyl-6-*O*-*tert*-butyldimethylsilyl-γ-CD [37]. These theoretical and experimental results suggest that the enantioselectivity depends on both the analyte structure and the type of derivatized CDs.

It is not trivial to correlate and predict enantiodiscrimination from the inherent properties of the analytes. Whereas the molecular dimensions of the analytes, the partial charges of the analyte substituents do not show correlation to the enantioselectivity, the dipole moments of the analytes do. The enantiodifferentiation increases with increasing dipole moment for the analytes bearing electron-withdrawing groups (CF_3, F, Cl and Br) excluding NO_2. For example, the enantioselectivity of CF_3-substituted analytes are in the order $o > m > p$, which corresponds to their dipole moments of 4.71, 4.54 and 3.36 Debye, respectively. For the same substituent position, the enantioselectivity is in the order $CF_3 > F > Cl > Br$, which is consistent with the dipole moment strength resulting from the electron-withdrawing ability of the substituents.

4. Conclusions

- Molecular docking, based on molecular mechanics calculations with AutoDock and semi-empirical PM3 calculations, has been carried out to predict enantiodiscrimination of styrene oxides by octakis(2,3-di-*O*-acetyl-6-*O*-*tert*-butyldimethylsilyl)-γ-cyclodextrin (DIACTGCD), through the differences in the interaction energies and inclusion geometries. The small binding free energy differences ($\Delta\Delta G$) obtained from AutoDock do not show any significant enantiodifferentiation. However, structure re-optimization with the PM3 method provides larger binding energy differences ($\Delta\Delta E$) and reveals that the degree of enantiodiscrimination was: $o > m > p$ for Cl-, CH_3- and CF_3-enantiomers; and $o > p > m$ for Br-, F- and NO_2-enantiomers.
- DIACTGCD exhibits a high discriminatory ability against the enantiomers of styrene oxides, implying a potential CSP for chromatographic chiral separation. DIACTGCD and styrene oxides have been synthesized and the GC analysis is proceeding. We believe that the complete GC analysis will provide results broadly but not entirely consistent with the results from these molecular docking calculations. The combined molecular docking and chromatographic results should then enable us to predict the enantioseparation and elution order of the other structurally related analytes on modified CD stationary phases.

Acknowledgements

We are grateful to the Computational Chemistry Unit Cell of the Department of Chemistry for computing facilities. We also thank Dr. Robert Butcher from the Publication Counseling Unit of the Faculty of Science for proof-reading the manuscript.

Appendix A. Supplementary data

Supplementary data associated with this article can be found, in the online version, at doi:10.1016/j.jmgm.2009.11.005.

References

[1] J. Szejtli, Introduction and general overview of cyclodextrin chemistry, Chem. Rev. 98 (1998) 1743–1753.
[2] E. Schneiderman, A.M. Stalcup, Cyclodextrins: a versatile tool in separation science, J. Chromatogr. B 745 (2000) 83–102.
[3] N.M. Maier, P. Franco, W. Lindner, Separation of enantiomers: needs, challenges, perspectives, J. Chromatogr. A 906 (2001) 3–33.
[4] V. Schurig, Separation of enantiomers by gas chromatography, J. Chromatogr. A 906 (2001) 275–299.
[5] J. Mosinger, V. Tománková, I. Němcová, J. Zýka, Cyclodextrins in analytical chemistry, Anal. Lett. 34 (2001) 1979–2004.
[6] Z. Juvancz, J. Szejtli, The role of cyclodextrins in chiral selective chromatography, Trends Anal. Chem. 21 (2002) 379–388.

[7] V. Schurig, Chiral separations using gas chromatography, Trends Anal. Chem. 21 (2002) 647–661.
[8] L. He, T.E. Beesley, Applications of enantiomeric gas chromatography: a review, J. Liq. Chromatogr. Relat. Technol. 28 (2005) 1075–1114.
[9] T.J. Ward, B.A. Baker, Chiral separations, Anal. Chem. 80 (2008) 4363–4372.
[10] A. Archelas, R. Furstoss, Synthesis of enantiopure epoxides through biocatalytic approaches, Annu. Rev. Microbiol. 51 (1997) 491–525.
[11] A. Steinreiber, K. Faber, Microbial epoxide hydrolases for preparative biotrans formations, Curr. Opin. Biotechnol. 12 (2001) 552–558.
[12] K.B. Lipkowitz, Atomistic modeling of enantioselection in chromatography, J. Chromatogr. A 906 (2001) 417–442.
[13] K.B. Lipkowitz, Applications of computational chemistry to the study of cyclodextrins, Chem. Rev. 98 (1998) 1829–1873.
[14] F. Kobor, K. Angermund, G. Schomburg, Molecular modelling experiments on chiral recognition in GC with specially derivatized cyclodextrins as selectors, J. High Resolut. Chromatogr. 16 (1993) 299–311.
[15] T. Beier, H.D. Höltje, Modified cyclodextrins as chiral selectors: molecular modelling investigations on the enantioselective binding properties of heptakis(2,3-di-*O*-methyl-6-*O*-*tert*.-butyldimethylsilyl)-β-cyclodextrin, J. Chromatogr. B 708 (1998) 1–20.
[16] M.C.K.V. Ramos, L.H.P. Teixeira, F.R. de Aquino Neto, E.J. Barreiro, C.R. Rodrigues, C.A.M. Fraga, Chiral separation of γ-butyrolactone derivatives by gas chromatography on 2,3-di-*O*-methyl-6-*O*-*tert*-butyldimethylsilyl-β-cyclodextrin, J. Chromatogr. A 985 (2003) 321–331.
[17] D.G. Durham, Application of force field calculations to the prediction of chirally discriminating chromatographic behaviour for β-CDs, Chirality 8 (1996) 58–66.
[18] C. Youngjin, J. Seunho, Molecular dynamics (MD) simulations for the prediction of chiral discrimination of *N*-acetylphenylalanine enantiomers by cyclomaltoheptaose (β-cyclodextrin, β-CD) based on the MM–PBSA (molecular mechanics–Poisson–Boltzmann surface area) approach, Carbohydr. Res. 339 (2004) 1961–1966.
[19] C. Youngjin, K. Dong Wook, P. Hyungwoo, H. Suntae, J. Karpjoo, J. Seunho, Prediction of chiral discrimination by β-cyclodextrins using grid-based Monte Carlo docking simulations, Bull. Korean Chem. Soc. 26 (2005) 769–775.
[20] C. Youngjin, K. Sung-Ryul, H. Suntae, J. Karpjoo, A grid computing-based Monte Carlo docking simulations approach for computational chiral discrimination, LNCS 3642 (2005) 446–455.
[21] G. Sicoli, Z. Jiang, L. Jicsinsky, V. Schurig, Modified linear dextrins (“acyclodextrins”) as new chiral selectors for the gas-chromatographic separation of enantiomers, Angew. Chem. Int. Ed. 44 (2005) 4092–4095.
[22] G. Sicoli, F. Pertici, Z. Jiang, L. Jicsinszky, V. Schurig, Gas-chromatographic approach to probe the absence of molecular inclusion in enantioseparations by carbohydrates. Investigation of linear dextrins (“acyclodextrins”) as novel chiral stationary phases, Chirality 19 (2007) 391–400.
[23] G. Sicoli, I. Tomoyuki, L. Jicsinszky, V. Schurig, A maltooctaose derivative (“acyclodextrin”) as a chiral stationary phase for enantioselective gas chromatography, Eur. J. Org. Chem. 25 (2008) 4241–4244.
[24] T. Aree, H. Hoier, B. Schulz, G. Reck, W. Saenger, Crystal structure of octakis(2,3,6-tri-*O*-methyl)-γ-cyclodextrin 4.5 H_2O: evidence for conformational flexibility of permethylated cyclodextrins, Carbohydr. Res. 328 (2000) 399–407.
[25] M.J. Frisch, G.W. Trucks, H.B. Schlegel, G.E. Scuseria, M.A. Robb, J.R. Cheeseman, J.A. Montgomery Jr., T. Vreven, K.N. Kudin, J.C. Burant, J.M. Millam, S.S. Iyengar, J. Tomasi, V. Barone, B. Mennucci, M. Cossi, G. Scalmani, N. Rega, G.A. Petersson, H. Nakatsuji, M. Hada, M. Ehara, K. Toyota, R. Fukuda, J. Hasegawa, M. Ishida, T. Nakajima, Y. Honda, O. Kitao, H. Nakai, M. Klene, X. Li, J.E. Knox, H.P. Hratchian, J.B. Cross, C. Adamo, J. Jaramillo, R. Gomperts, R.E. Stratmann, O. Yazyev, A.J. Austin, R. Cammi, C. Pomelli, J.W. Ochterski, P.Y. Ayala, K. Morokuma, G.A. Voth, P. Salvador, J.J. Dannenberg, V.G. Zakrzewski, A.D. Daniels, O. Farkas, A.D. Rabuck, K. Raghavachari, J.V. Ortiz, Gaussian 03, Gaussian Inc., Pittsburgh, PA, USA, 2004 .
[26] G.M. Morris, D.S. Goodsell, R.S. Halliday, R. Huey, W.E. Hart, R.K. Belew, A.J. Olson, AutoDock, Version 4.0.1, The Scripps Research Institute, La Jolla, CA, USA, 2007.
[27] M.F. Sanner, R. Huey, S. Dallakyan, S. Karnati, W. Lindstrom, G.M. Morris, B. Norledge, A. Omelchenko, D. Stoffler, G. Vareille, AutoDockTools, Version 1.4.5, The Scripps Research Institute, La Jolla, CA, USA, 2007.
[28] J. Gasteiger, M. Marsili, Iterative partial equalization of orbital electronegativity—a rapid access to atomic charges, Tetrahedron 36 (1980) 3219–3228.
[29] W.H. Pirkle, T.C. Pochapsky, Considerations of chiral recognition relevant to the liquid chromatographic separation of enantiomers, Chem. Rev. 89 (1989) 347–362.
[30] D.E. Koshland Jr., Protein shape and biological control, Sci. Am. 229 (1973) 52–64.
[31] J.H. Reibenspies, D.K. Maynard, A. Derecskei-Kovacs, G. Vigh, Crystal structures of heptakis(2,6-di-*O*-*tert*butyldimethylsilyl)-cyclomaltoheptaose, heptakis(2-*O*-methyl-3,6-di-*O*-*tert*-butyldimethylsilyl)-cyclomaltoheptaose and heptakis(2-*O*-methyl)-cyclomaltoheptaose, Carbohydr. Res. 328 (2000) 217–227.
[32] M. Katoh, S. Kohmoto, K. Kishikawa, A hexagonal columnar packing structure of C7 symmetric supramolecules: a superstructure of a 2:3 complex of heptakis-(6-O-tert-butyldimethylsilyl)-β-cyclodextrin and ethyl acetate, Cryst. Res. Technol. 41 (2006) 1242–1245.
[33] C.E. Dalgliesh, The optical resolution of aromatic amino-acids on paper chromatograms, J. Chem. Soc. 137 (1952) 3940–3942.
[34] S. Ahn, J. Ramirez, G. Grigorean, C.B. Lebrilla, Chiral recognition in gas-phase cyclodextrin: amino acid complexes—is the three point interaction still valid in the gas phase? J. Am. Soc. Mass Spectrom. 12 (2001) 278–287.
[35] K.B. Lipkowitz, D.A. Demeter, R. Zegarra, R. Larter, T. Darden, Protocol for determining enantioselective binding of chiral analytes on chiral chromatographic surfaces, J. Am. Chem. Soc. 110 (1988) 3446–3452.
[36] J.L. Anderson, J. Ding, R. McCulla, W.S. Jenks, D.W. Armstrong, Separation of racemic sulfoxides and sulfinate esters on four derivatized cyclodextrin chiral stationary phases using capillary gas chromatography, J. Chromatogr. A 946 (2002) 197–208.
[37] T. Eisuke, E. Karl-Heinz, 2,3-Di-*O*-methoxymethyl-6-*O*-*tert*-butyldimethylsilyl-γ-cyclodextrin: a new class of cyclodextrin derivatives for gas chromatographic separation of enantiomers, J. Chromatogr. A 1063 (2005) 181–192.